Chiral Symmetry Breaking and Polymorphism in 1,1′-Binaphthyl Melt Crystallization

C. Ignacio Sainz-Díaz,* Africa P. Martín-Islán, and Julyan H. E. Cartwright

Laboratorio de Estudios Cristalográficos, Instituto Andaluz de Ciencias de la Tierra (CSIC)—Edificio BIC Granada, Avenida de la Innovacion, 1, P.T. Ciencias de la Salud, E-18100 Armilla, Granada, Spain

Received: April 8, 2005; In Final Form: August 1, 2005

We have studied chiral symmetry breaking in the melt crystallization of 1,1′-binaphthyl. We confirm that chiral symmetry breaking can be induced by stirring the melt as it crystallizes. We find an additional process of vapor crystallization to occur alongside the melt crystallization. This complicates the analysis of the enantiomorphism by introducing a further phenomenon: that of polymorphism. Crystallographic studies by X-ray diffraction reveal two polymorphs of 1,1′-binaphthyl that are made up of two different conformers of each of the two enantiomeric forms of the molecule. Crystals from the melt are generally chiral tetragonal crystals ($P42_12_1$) composed of (*R*)- or (*S*)-1,1′-binaphthyl in a transoid conformer, while those from the vapor are racemic monoclinic crystals ($C2/c$) made up of the cisoid conformer of both (*R*)- and (*S*)-1,1′-binaphthyl enantiomers. The main intermolecular interactions in all these crystals are weak aromatic CH/π hydrogen bonds, which are responsible for the enantiomeric discrimination in the molecular recognition during crystallization. A tendency for whisker crystal formation is notable in 1,1′-binaphthyl. In stirred crystallization, fluid and mechanical forces can break off these whiskers, which provide secondary nuclei for further crystallization. This autocatalytic mechanism induces chiral symmetry breaking during the crystallization.

Introduction

The derivatives of 1,1′-binaphthyl are well-known from their applications as chiral recognition receptors and chiral catalysts.[1] The rotation about the σ-bond of 1,1′-binaphthyl and its derivatives is so hindered that optical isomers may be isolated (Figure 1). In the nonsubstituted case, this barrier is low enough that 1,1′-binaphthyl racemizes spontaneously in solution at room temperature in some hours[2] and in the melt at 180 °C in seconds,[3] but in substituted binaphthyls it can be much higher. The rotational barrier plays a fundamental role in the discriminating ability of 1,1′-binaphthyls in enantiomeric reactions and chiral recognition. The dihedral angle θ between the two naphthyl planes is an important quantity for describing the chiral properties of 1,1′-binaphthyl and its derivatives. X-ray diffraction studies of nonsubstituted 1,1′-binaphthyl[4] in crystalline form have revealed the presence of two conformers of each enantiomer: a cisoid variety with $\theta = 68^{5,6}-98.8°$,[1,7] and another, transoid, form with $\theta = 103°$.[5,8] Although the rotational barrier has been studied both experimentally[1,2] and theoretically,[1,5] there remain some discrepancies, as in the literature some authors describe two minimum energy states with θ values of 55−70° and 105−130°,[1] whereas other authors find only one minimum.[1,5]

Chiral symmetry breaking has been observed in the crystallization of both inorganic[9] and organic compounds.[3,10] This process can be induced by seeding with a chiral compound[11] or by stirred crystallization. The latter phenomenon has been observed during the stirred crystallization of sodium chlorate from solution[9] and in the stirred melt crystallization of 1,1′-binaphthyl.[3] In previous work[12] we clarified the mechanism of chiral symmetry breaking during crystallization. We showed with numerical simulations and theoretical arguments that secondary nucleation—nucleation of new crystals caused by the presence of an existing primary crystal—is a nonlinear autocatalytic process capable of explaining the chiral symmetry breaking.

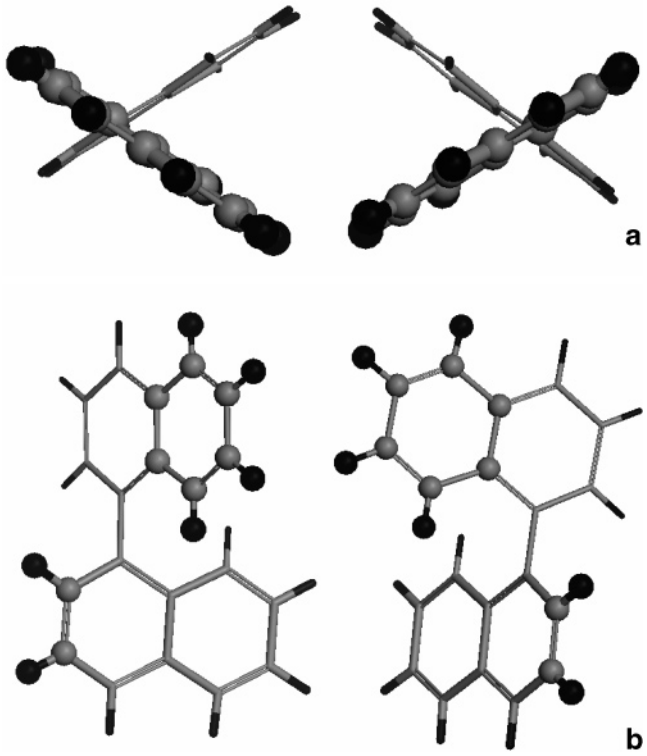

Figure 1. Chirality in the molecular structure of 1,1′-binaphthyl seen from two different viewpoints (the parts in the foreground are in the ball-and-stick style).

To nucleate a crystal requires overcoming a certain energy barrier. The height of this barrier is a function of the concentration of a solution or the temperature of a melt. A supersaturated solution concentrated beyond its saturation point, or a super-

* Corresponding author. E.mail: sainz@lec.ugr.es.

10.1021/jp0518198 CCC: $30.25
Published on Web 09/20/2005

cooled melt cooled beyond its freezing point, are systems metastable to nucleation. With a solid surface already present, less energy is required to surmount the barrier. Thus functions secondary nucleation, in which the presence of one crystal facilitates the production of further crystals. Secondary nucleation can act as a nonlinear autocatalytic process, since, in the case of chiral crystallization, secondary nuclei possess the same chirality as that of the mother crystal, so the presence of a crystal of a given chirality catalyses the production of further crystals with the same chirality. Secondary nucleation has been extensively investigated, particularly for its relevance to industrial crystallization.[13,14] The mechanism on the microscale of homochiral secondary nucleation necessarily involves the surface of the mother crystal. Contact nucleation, in which collisions between one crystal and another, or between a crystal and the fluid boundaries (container walls, stirring bar, etc.), break pieces off the surface, and fluid shear, which may also detach fragments from the crystal surface, are two mechanisms for homochiral secondary nucleation.[15,16] Both of these mechanisms involve the production and subsequent removal of relatively weakly attached homochiral material from the crystal surface. For either mechanical or fluid forces to break material off from the growing crystal surface, that material must be relatively weakly attached, which implies that the surface must be rough, rather than smooth. While crystals at low supersaturations or supercoolings grow by the addition of material at the edges of smooth layers (so-called tangential growth), at increasing supersaturations or supercoolings the surface grows in a more disordered manner (normal growth).[17] It is clear that the larger the number and size of asperities on the crystal surface, the greater the probability of detaching fragments by mechanical shock or fluid shear. The detached pieces will possess the same chirality as the mother crystal of which they previously formed a part. At the highest supersaturations or supercoolings, these asperities can be the result of normal growth, but even with tangential growth at more moderate supersaturations or supercoolings it is possible to have structures that are easily detached. Whisker crystals are an example. In this crystal-growth morphology, long thin crystallites, or whiskers (defined as crystals with aspect ratio greater than 10:1), grow out from the substrate beneath.

In previous work we showed the presence of these whisker crystals in binaphthyl crystallization.[12] Here we report in detail our findings regarding crystallizing 1,1′-binaphthyl from the melt.

Experimental Section

We carried out crystallizations using 1,1′-binaphthyl commercially available from Acros Inc. We performed a similar procedure to that previously reported[3,18] using varying amounts of reagent from 0.02 to 1 g. We tested different containers including sealed and open, and narrow and wide flasks (vide infra). In all cases we placed the container with the sample in a bath of silicone oil and heated it to 180 °C, melting the solid for 20 min to be sure that the whole sample had racemized completely. We then cooled the melt to 150 °C and allowed it to crystallize. In each experiment we performed two runs simultaneously: one with magnetic stirring using a small Teflon stir-bar in the flask and the other without stirring.

We performed the optical rotation measurements at $\lambda = 598$ nm with a standard automatic polarimeter in a 1 cm cell at room temperature after dissolving the solids in chloroform. Under these conditions we found the racemization half-life of 1,1′-binaphthyl to be about 24 h. In those cases where the light transmittance was too low for the polarimeter, we pretreated the sample with powdered active carbon for 15 min at room temperature. We found this treatment to have a negligible effect on the optical rotation. We performed the differential scanning calorimetry analyses using a Shimazdu DSC-50 calorimeter in an aluminum cell with air atmosphere with a rate flow of 100.0 mL/min and a constant heating rate of 2 °C/min. The powder X-ray diffraction analysis we carried out with a Phillips diffractometer. We performed the scanning electron microscopy studies using a C. ZEISS DSM 950 microscope, after protecting the samples with vapor deposition of a thin layer of gold.

Results and Discussion

We carried out preliminary trials to optimize the amount of sample for the crystallization experiments. Pincock et al.[18] used 20 mg of 1,1′-binaphthyl per trial and found a broad Gaussian distribution of the specific rotation of the crystallized products with a very high proportion of experiments with low optical rotation; the yield of a 1,1′-binaphthyl with high optical rotation being an exceptional event. Recently Kondepudi et al.[3] reported the preparation of 1,1′-binaphthyl with high optical rotation by using 2 g of sample in each test. In the current work, we explored the use of differing amounts of 1,1′-binaphthyl from 20 mg to 1 g. The trials with 20 mg of 1,1′-binaphthyl did not show large optical rotation differences between stirred and nonstirred runs. We found that the use of 0.5−1 g of 1,1′-binaphthyl in each crystallization trial was sufficient to yield a product with high optical rotation.

During our trials of different sizes of reactor vessel for the melt crystallization, we observed an additional process: the evaporation and recrystallization of 1,1′-binaphthyl from the vapor in the top part of the reactor. This behavior is consistent with the vapor−solid process reported previously, where a polymorph transformation was observed in this compound.[8] However, this phenomenon has not been reported previously in this kind of stirring melt crystallization experiments, and it is noteworthy because the crystals formed from the vapor can drop down and mix with the melt crystals, altering the results. We found that the vapor crystallizes in the sealed top and on the walls of the reactor, forming long white needles. We settled on a 3 cm diameter vessel for the crystallization, in which this crystal condensation was less than in narrower reactors. In all cases, the proportion of these crystals from vapor recollected was lower than 10% of the initial solid, although these crystals are fixed very weakly to the reactor walls and the proportion of crystals dropped down could be higher during the experiments. Runs in open reactors presented fewer crystals formed from the vapor than runs performed in sealed reactors. In both open and sealed reactors, the stirred runs gave far fewer crystals from the vapor than the unstirred runs. In all trials, we separated the crystals from the vapor from the crystals from the melt, and we analyzed them separately and compared one with the other.

The solids obtained from the melt in unstirred runs show very low optical rotation ($\alpha < \pm 10°$). There was more variation in trials using samples of less than 0.5 g, which is to be expected as random fluctuations about the mean are more significant in a small sample. All crystals formed from the vapor present no optical rotation ($\alpha = 0°$). The solids obtained from the melt in the stirred open reactor display high optical rotation ($\pm 150° < \alpha < \pm 200°$), whereas the solids obtained from the melt in stirred sealed reactors show lower optical rotation with a greater variability between trials. We surmise this to be due to contamination by crystals from the vapor dropping into the melt in the sealed reactor. This hypothesis explains the minimum amount of initial sample we found necessary to obtain chiral

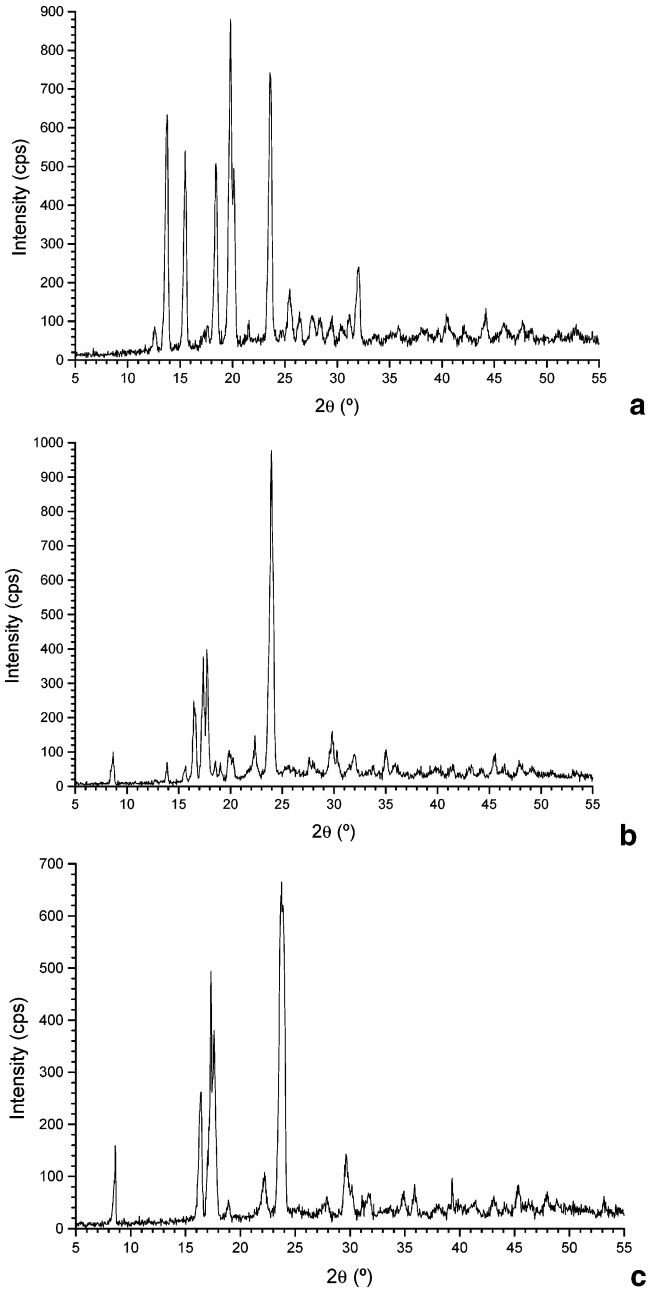

Figure 2. Powder X-ray diffraction patterns of 1,1′-binaphthyl crystallized from (a) the melt in stirred trials, (b) the melt in unstirred trials, and (c) vapor.

symmetry breaking. Starting with a too small amount of sample, the proportion of crystals from the vapor is significant with respect to those from the melt, whereas this proportion is much smaller and does not greatly alter the optical rotation of the melt crystals when a large initial amount of sample is used. For the same reason, in stirred trials with a small amount of sample (<0.5 g) the enantiomeric excess was lower than with 0.5−1 g of sample.

Powder X-ray diffraction studies of the solids reveal the presence of different crystalline structures among the recovered solids. Crystals from the melt in stirred trials show similar X-ray diffraction patterns in all cases (Figure 2a). Solids from unstirred runs, from the melt, and from the vapor, present different powder X-ray diffraction patterns (Figure 2, parts b and c), depending on the temperature distribution in the melt and at the top of the reactor. This demonstrates the existence of polymorphism in this crystallization. For comparisons with previous crystal-

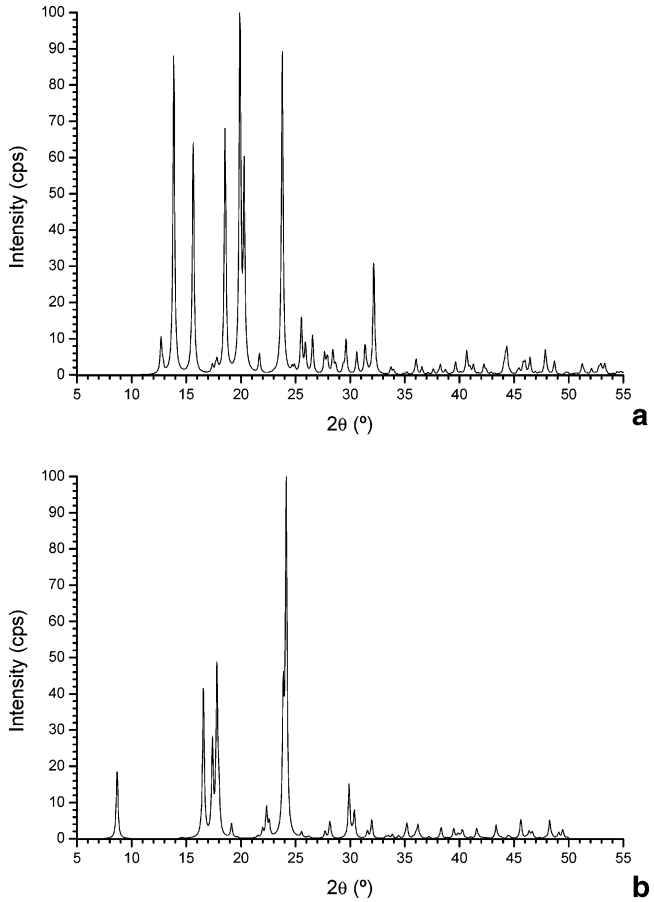

Figure 3. Powder X-ray diffraction patterns simulated from crystal structures obtained previously from a single crystal: (a) chiral form $P4_12_12_1$ and (b) racemic form $C2/c$.

lographic data of 1,1′-binaphthyl, we performed powder X-ray diffraction pattern simulations using diffraction software implemented within the Cerius2 package (from Accelrys Inc.) with an X-ray wavelength of 1.54 Å and a 2θ range of 5−55°. Chiral crystals obtained from stirred melt crystallization present the same powder X-ray diffraction pattern as that simulated (Figure 3a) from the single-crystal structure of transoid 1,1′-binaphthyl[7,8] that corresponds to a $P4_12_12_1$ tetragonal polymorph, while crystals from the vapor with no optical activity present a similar powder X-ray diffraction pattern to that simulated from the single-crystal structure of cisoid 1,1′-binaphthyl (Figure 3b) corresponding to a racemic monoclinic $C2/c$ form.[8] Solids from the melt tend to crystallize in the $P4_12_12_1$ form with a large enantiomeric excess in stirred runs and a smaller enantiomeric excess in unstirred runs. However, in some trials a certain number of $C2/c$ crystals were found in the solids formed from the melt along with the $P4_12_12_1$ crystals. We interpret this as arising from a temperature gradient inside the reactor,[19] which can be large enough to allow the formation of the $C2/c$ polymorph in the low-temperature zones. This occurrence was more frequent in unstirred runs—only the $C2/c$ form was obtained in some trials—in which the temperature equilibration is slower than in stirred runs. The racemic crystals ($C2/c$) tend to appear in solids obtained from the vapor. However, when the temperature of the top of reactor was high enough, a conglomerate of $P4_12_12_1$ crystals was formed there along with the $C2/c$ crystals. We examined the polymorph mixtures with a quantitative powder X-ray diffraction analysis using XPOWDER software[20] in order to distinguish the polymorphism and the symmetry-breaking phenomena.

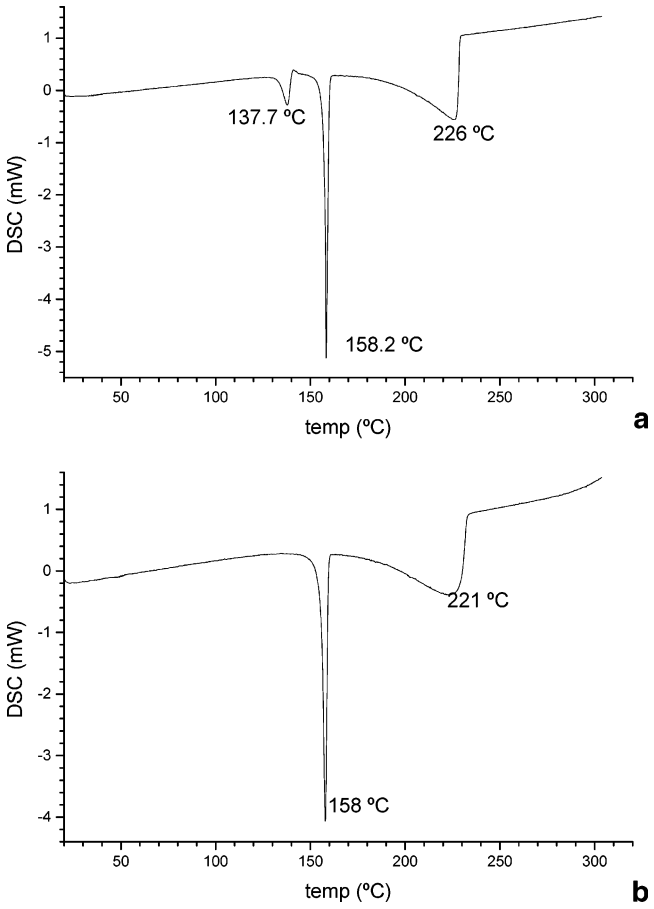

Figure 4. Differential scanning calorimetry profile of solid obtained from vapor in (a) an unstirred run and (b) from melt in a stirred run.

Differential scanning calorimetry studies of these solids reveal them to have different thermal behaviors. Solids from unstirred runs, from melt, and vapor, whose powder X-ray diffraction analysis shows the presence of racemic crystals (*C*2/*c*), have thermal profiles (Figure 4a) with three endothermic troughs around 138 °C (a broad trough, 132−143 °C), 158 °C (a deep narrow trough), and 222−226 °C (a very broad trough, 170−232 °C). The crystals from the melt in stirred runs do not show the endothermic trough at 138 °C but do present the troughs at 158 and 222−226 °C (Figure 4b). The endothermic trough at 158 °C corresponds to the melting process of the $P4_12_12_1$ form with a fusion enthalpy of approximately 66−75 J/g (4.6 kcal/mol) similar to values previously reported.[21] The broad endothermic trough at 222−226 °C corresponds to the evaporation process of 1,1′-binaphthyl with a vaporization enthalpy of 0.2−0.3 kJ/g. This evaporation process starts slowly at 130 °C, increases significantly after 160 °C, and finishes abruptly at 230 °C, with the minimum of the thermal profile at 222−226 °C in all cases. This explanation is confirmed by thermogravimetric data that show that the mass loss is negligible at 130−160 °C, while being important at higher temperatures. This analysis explains the evaporation of 1,1′-binaphthyl observed during the crystallization trials. The thermal behavior of racemic (*C*2/*c*) crystals at 130−145 °C displays two overlapping processes: an initial melting of the crystals showing an endothermic trough and an exothermic recrystallization forming the chiral crystal ($P4_12_12_1$) that disguises the real intensity of the melting trough, neutralizing it and leaving a small exothermic peak. This profile is typical of a monotropic system[22] in which the melting of the *C*2/*c* form takes place concomitantly with its transformation into the crystal form $P4_12_12_1$. This hypothesis justifies the low position of the minimum observed for the melting trough of the *C*2/*c* form (at 137−139 °C instead of 145 °C[8]) and the low value of the apparent fusion enthalpy observed (10−21 J/g) with respect to the $P4_12_12_1$ form. These results bear on the discussion that exists in the literature about the nature of the transformation in such cases; whether it is a solid-state process or a solid−liquid−solid or solid−vapor−solid process.[8,21] The low-temperature rate (2 °C/min) in the DSC analysis allows us to show for first time that the formation of the $P4_12_12_1$ form starts before the melting process finishes. We hypothesize that the *C*2/*c* form starts to become a disordered or glassy solid at 137−139 °C. This situation allows a rearrangement of the molecules for packing in the $P4_12_12_1$ form and initiates the formation of this polymorph before the melting process is complete. We hypothesize that a solid-state transformation could best explain this behavior. In a standard melting point analysis when the temperature increase is fast enough, the *C*2/*c* solid can be transformed in a liquid as a metaestable phase that will transform later in a $P4_12_12_1$ crystal at the temperature of the melting point.

The observed packing of the cisoid 1,1′-binaphthyl conformer is as an achiral crystal (*C*2/*c*) in which the lattice unit is comprised of two molecules of the R enantiomer and another two of the S enantiomer (Figure 5, parts a and b). However, the transoid 1,1′-binaphthyl conformer is found in chiral crystals ($P4_12_12_1$) comprised solely of the R or S enantiomer (Figure 5c). Thus, in the achiral crystals the 1,1′-binaphthyl molecule always adopts a cisoid conformation with a dihedral angle of 68.6°, whereas the chiral crystals always have 1,1′-binaphthyl molecules in a transoid conformation with a dihedral angle of 103°. In both cases the intermolecular interactions are mainly electrostatic—weak hydrogen bonds—between the H atoms and the π electronic charge from the aromatic rings. In both chiral and achiral crystals the aromatic rings of vicinal molecules are parallel, but they are shifted in such way that only the H atoms are close to the π electrical field of the aromatic ring. In the achiral crystal the cisoid conformers form racemic pairs. Probably this molecular packing and the intermolecular interactions force the molecule to adopt the cisoid conformation. On the other hand there are no racemic pairs in the chiral crystal; the molecular packing yields a lower density (1.18 g cm^{-3}) than the achiral crystal (1.28 g cm^{-3}) and allows the transoid conformation in the molecules.

Thus the achiral *C*2/*c* crystal is not a conglomerate of chiral $P4_12_12_1$ crystals but a racemic crystal, an optically inactive polymorph. The chiral $P4_12_12_1$ crystal has a higher melting point than the racemic *C*2/*c* version. This may indicate that the $P4_12_12_1$ form is more stable in terms of free energy, although it is less dense, than the *C*2/*c* polymorph. This achiral form is thermodynamically more stable at low temperature than the chiral one according to previous results.[21] However, at high temperature the $P4_12_12_1$ form is more stable than the achiral *C*2/*c* form. Besides, the entropy of both polymorphs should be different. Probably the packing together of the R and S enantiomers for forming the *C*2/*c* crystal will require an additional ordering, and the entropy of the *C*2/*c* form will be lower than in $P4_12_12_1$ form. Therefore, an increase of temperature will increase the entropic term, and the $P4_12_12_1$ form will have a lower free energy than the achiral one. The achiral crystal achieves a more efficient packing of the molecules than the chiral one, but the intermolecular interactions in the $P4_12_12_1$ form are stronger than in the *C*2/*c* form. The distance between the hydrogen and the closest aromatic carbon of the facing π ring is 2.89 and 2.96 Å in $P4_12_12_1$ and *C*2/*c* crystals, respectively. Although the energy of the weak aromatic CH/π hydrogen bonds, which provide the

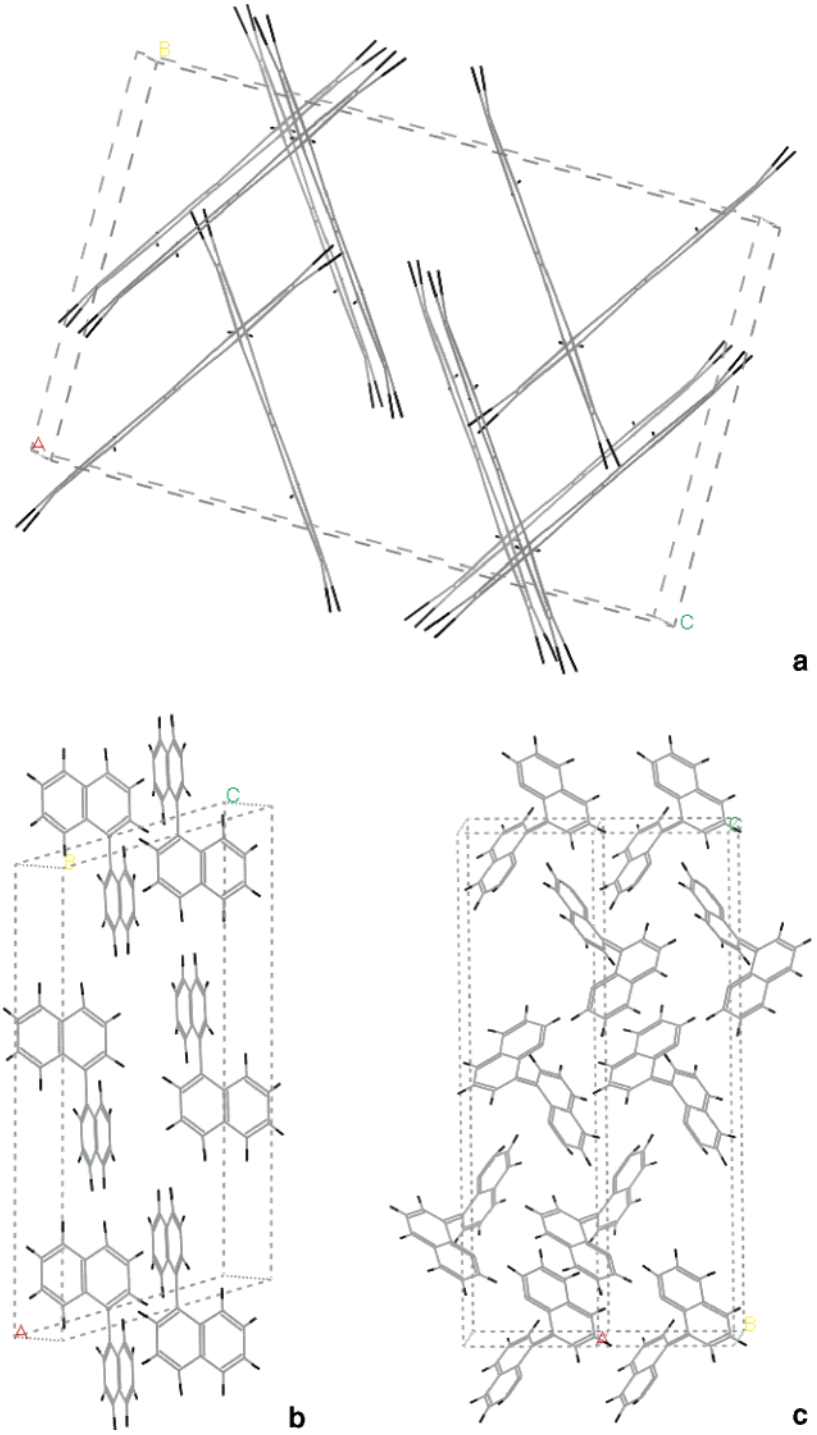

Figure 5. Molecular packing in the *C*2/*c* (a and b) and $P42_12_1$ (c) polymorphs of 1,1′-binaphthyl.

main intermolecular interactions in these crystals, is small, the enthalpy difference in the crystal lattice may become appreciable as a result of the interplay of many intermolecular interactions. These aromatic CH/π interaction plays an important role in crystal packing of clathrates and other structures, in solid-state reactions, and in the mechanism of enantiomeric discrimination or resolution.[23] Compounds with large π-surfaces, such as those containing naphthyl groups, are often more effective in enantiomeric discrimination during crystallization than their phenyl analogues. This is the basis of the application of 1,1′-binaphthyl derivatives as enantioselective catalysts.

The crystallization of 1,1′-binaphthyl from the condensation of vapor—at the top of the reactor—yielded the achiral *C*2/*c* polymorph when the surface temperature was lower than 140 °C. This fact is presumably due to the achiral form being more stable than the chiral one at low temperatures. However, when the surface temperature is high enough, the crystallization from vapor yields the chiral $P42_12_1$ form obtaining an optically inactive conglomerate of chiral crystals. The formation of the *C*2/*c* polymorph is thus independent of the stirring procedure but is dependent on the temperature gradient in the reactor, according to previous results.[19]

We explored the morphologies of the crystals with scanning electron microscopy. We observed the formation of whisker crystals in the solids obtained by condensation from vapor (Figure 6a). The propensity of 1,1′-binaphthyl to generate such whisker crystals can be appreciated also during its crystallization from the melt. The scanning electron microscope pictures of

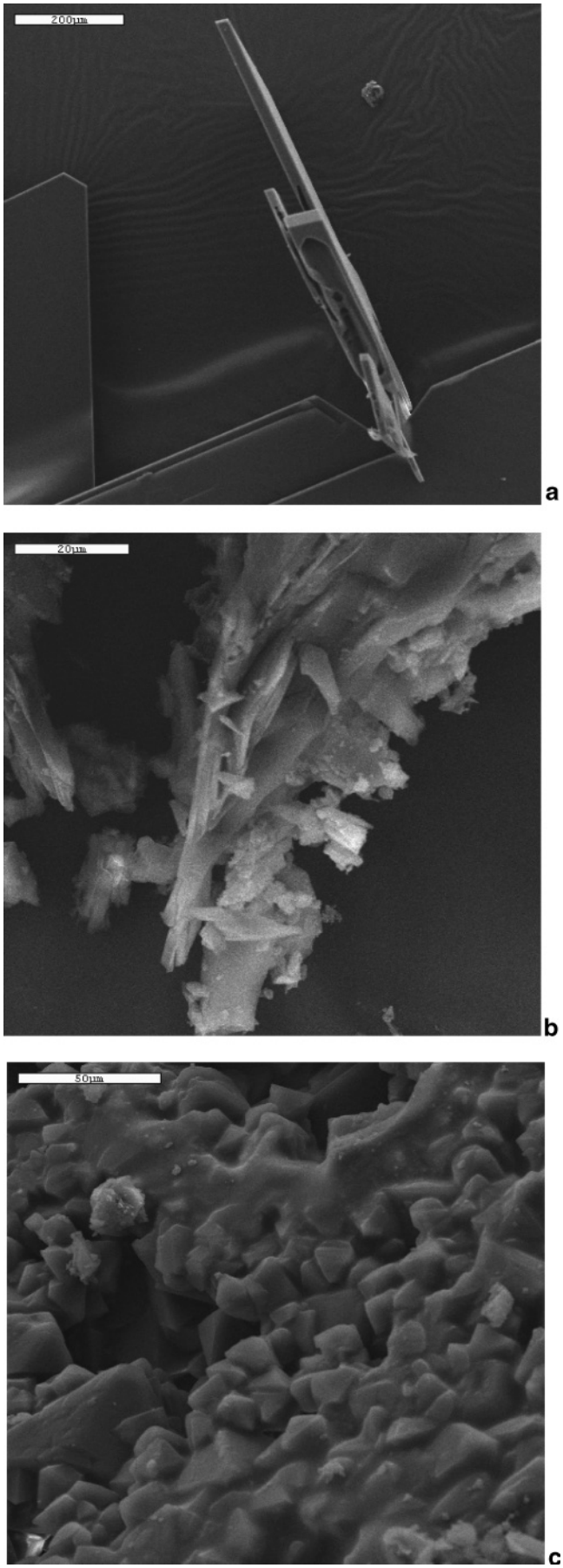

Figure 6. Scanning electron microscope pictures of the solids formed from vapor (a) and from melt crystallization in unstirred (b) and stirred (c) trials.

the solid crystallized from the unstirred melt show remains of small whiskers and thin plates (Figure 6b). The fluid and mechanical forces existing in stirred crystallization can break off these whiskers, as their shape makes them easy to detach from the primary crystal, and they can then act as secondary nuclei. These homochiral nuclei are dispersed by the fluid dynamics of the stirring regime. The scanning electron microscope pictures of the solid crystallized from the stirred melt show that neither whiskers nor any other weakly attached forms remain after the stirring (Figure 6c). As we showed in earlier work, both with theoretical arguments and with simulations, it is whiskers and other similar asperities on the crystal surfaces that provide the microscopic mechanism for chiral symmetry breaking during the crystallization by acting as homochiral secondary nuclei after dispersal throughout the fluid.

Conclusions

In the crystallization of 1,1′-binaphthyl from the melt, chiral symmetry breaking is produced by stirring. The direction of stirring is not important—one sense does not produce one enantiomer, and the opposite sense, the other—unlike in experiments on larger molecules that stack together to form chiral mesoscale structures which are susceptible to macroscopic hydrodynamic interactions, in which the chirality does depend on the direction of stirring.[24]

In addition to chiral symmetry breaking, polymorphism is also present in this system. As well as the chiral tetragonal ($P42_12_1$) polymorph of 1,1′-binaphthyl, found in either one or other or both of its enantiomorphs according to the symmetry breaking in the solids deposited from the melt, we also find achiral racemic monoclinic ($C2/c$) crystals of another polymorph of 1,1′-binaphthyl in solids deposited from the vapor in the upper part of the reactor and at low temperatures in solids formed from the melt. However, the formation of the $C2/c$ polymorph is only dependent on the temperature profile and is independent of the stirring process. These experiments and our thermal analysis at low-temperature rate reveal that the polymorph transformation can happened following the vapor−solid process and also through a solid-state process depending on the experimental conditions. This result will clarify the discussion found in the literature about the nature of this transformation.[8,21]

The physical mechanism of chiral symmetry breaking is by secondary nucleation. It has recently been postulated that in 1,1′-binaphthyl crystallization—in connection with the small enantiomeric excess obtained in some stirred runs—that R nuclei may form on an S crystal surface and vice versa.[25] We maintain that this is not likely; that secondary nucleation is a mechanism that preserves homochirality, and that the degree of chiral purity in the final products of stirred 1,1′-binaphthyl crystallization depends on the extent of the contamination of the melt by vapor-deposited crystals falling in, together with the efficiency of the stirring in producing symmetry breaking via mechanical and fluid forces. We conclude that the physical process leading to this secondary nucleation in a stirred crystallization is that the stirring process causes pieces to break off the initial crystals, producing seeds for autocatalytic secondary nucleation, and the stirring process itself does not produce the secondary nucleation as reported previously.[26]

Acknowledgment. The authors are grateful to Dilip Kondepudi for useful information and to J. Daniel Martín-Ramos for fruitful discussions and for the Xpowder software. We acknowledge the financial support of the Spanish CSIC (A. Martín-

Islán), the Spanish MCYT, and the FEDER Fund of the European Union (Grants PPQ2001-2932 and CTQ2004-04648).

References and Notes

(1) Setnicka, V.; Urbanova, M.; Bour, P.; Kral, V.; Volka, K. *J. Phys. Chem.* **2001**, *105*, 8931−8938.

(2) Colter, A. K.; Clemens, L. M. *J. Phys. Chem.* **1964**, *68*, 651.

(3) Kondepudi, D. K.; Laudadio, J.; Asakura, K. *J. Am. Chem. Soc.* **1999**, *121*, 1448−1451.

(4) Pauptit, R. A.; Trotter, J. *Can. J. Chem.* **1983**, *61*, 69.

(5) Kranz, M.; Clark, T.; Schleyer, P.v. R. *J. Org. Chem.* **1993**, *58*, 3317−3325.

(6) Kerr, K. A.; Robertson, J. M. *J. Chem. Soc. B* **1969**, 1146.

(7) Kuroda, R.; Mason, S. F. *J. Chem. Soc., Perkin Trans. 2* **1981**, 167.

(8) Kress, R. B.; Duesler, E. N.; Etter, M. C.; Paul, I. C.; Curtin, D. *J. Am. Chem. Soc.* **1980**, *102*, 7709.

(9) Kondepudi, D. K.; Sabanyagam, C. *Chem. Phys. Lett.* **1994**, *217*, 364−368.

(10) Soai, K.; Sato, I.; Shibata, T.; Komiya, S.; Hayashi, M.; Matsueda, Y.; Imamura, H.; Hayse, T.; Morioka, H.; Tabira, H.; Yamamoto, J.; Kowata, Y. *Tetrahedron: Asymmetry* **2003**, *14*, 185−188.

(11) Buhse, T.; Kondepudi, D. K.; Hoskins, B. *Chirality* **1999**, *11*, 343−348.

(12) Cartwright, J. H. E.; García-Ruiz, J. M.; Piro, O.; Sainz-Díaz, C. I.; Tuval I. *Phys. Rev. Lett.* **2004**, *93*, 033502.

(13) Strickland-Constable, R. F. *Kinetics and Mechanism of Crystallization*; Academic Press: London, 1968.

(14) Nývlt, J.; Söhnel, O.; Matuchová, M.; Broul, M. *The Kinetics of Industrial Crystallization*; Elsevier: Amsterdam, 1985.

(15) Martin, B.; Tharrington, A.; Wu, X. I. *Phys. Rev. Lett.* **1996**, *77*, 2826.

(16) Buhse, T.; Durand, D.; Kondepudi, D.; Laudadio, J.; Spilker S. *Phys. Rev. Lett.* **2000**, *84*, 4405.

(17) Chernov, A. A. *J. Struct. Biol.* **2003**, *142*, 3.

(18) Pincock, R. E.; Perkins, R. R.; Ma, A. S.; Wilson, K. R. *Science* **1971**, *174*, 1018−1020.

(19) Asakura, K.; Nagasaka, Y.; Hidaka, M.; Hayashi, M.; Osanai, S.; Kondepudi, D. K. *Chirality* **2004**, *16*, 131−136.

(20) Martin, J. D. *XPowder*. Quantitative and Qualitative Powder X-ray Diffraction Analysis, version 2004.03; http://www.xpowder.com; Orión Network Communication: Granada, 2004.

(21) Wilson, K. R.; Pincock, R. E. *J. Am. Chem. Soc.* **1975**, *97*, 1474−1478.

(22) Jaques, J.; Mollet, A.; Wilen, S. M. *Enantiomers, Racemates, and Resolutions*; Wiley: New York, 1981.

(23) Suezawa, H.; Ishihara, S.; Umezawa, Y.; Tsuboyama, S.; Nishio M. *Eur. J. Org. Chem.* **2004**, 4816−4822.

(24) Ribó, J. M.; Crusats, J.; Sagués, F.; Claret, J.; Rubires, R. *Science* **2001**, *292*, 2063.

(25) Asakura, K.; Nagasaka, Y.; Osanai, S.; Kondepudi, D. K. *J. Phys. Chem. B* **2005**, *109*, 1586−1592.

(26) Kondepudi, D. K.; Asakura, K. *Acc. Chem. Res.* **2001**, *34*, 946−954.